

## REFRACTIVE INDEX AND THICKNESS EVALUATION OF MONOMODE AND MULTIMODE STEP-INDEX PLANAR OPTICAL WAVEGUIDES USING LONGITUDINAL SECTION MAGNETIC (LSM) AND LONGITUDINAL SECTION ELECTRIC (LSE) FORMULATION

Adrián F. Gavela<sup>1</sup>, Silvino J. A. Presa<sup>1</sup>, Miguel G. Granda<sup>1</sup>, Isabel A. Martos<sup>2</sup>, María T. F. Abedul<sup>2</sup>, Agustín C. García<sup>2</sup>, María R. Lastra<sup>3</sup>, and José R. García<sup>1,\*</sup>

<sup>1</sup>Physics Department, University of Oviedo, Oviedo, Spain

<sup>2</sup>Physical and Analytical Chemistry Department, University of Oviedo, Oviedo, Spain

<sup>3</sup>Energy Department, University of Oviedo, Oviedo, Spain

**Abstract**—In this work, we demonstrate that the LSM and LSE modes formulation is an excellent theoretical tool for determining the refractive index and thickness of the guiding layer in planar optical waveguides with step refractive index profile. Refractive index of transparent materials capable of being deposited as a solid thin layer on a substrate for confining light can be evaluated very accurately. The method can be applied to analyze and design monomode and multimode optical waveguides, unlike the methods proposed so far, including cutoff wavelength region. This wave model only requires the experimental evaluation of the effective indices of the guided modes. In order to verify the developed formulation, the commercial software Olympios was used for theoretical comparison. Polymeric planar optical waveguides were fabricated and characterized. A prism coupling method and the Metricon system were used for effective indices measurements and to compare the accuracy. The experimental evaluation of the thickness was carried out by profilometry. In all cases a complete agreement was obtained for refractive index and thickness between theory and experiments.

---

*Received 26 October 2012, Accepted 26 November 2012, Scheduled 29 November 2012*

\* Corresponding author: José Rodríguez García (jose@uniovi.es).

## 1. INTRODUCTION

The motivation for this work arises from the joint research between the Immunoanalysis (Physical and Analytical Chemistry Department) and Integrated Optics (Physics Department) laboratories of the University of Oviedo. In this collaboration, Match Zehnder Interferometers (MZI) with polymeric channel optical waveguides in glass substrates are being investigated for biosensing applications. Since the sensing action is performed by the interaction of the analyte with the evanescent electromagnetic field of the guided light, the accurate knowledge of the refractive index of the polymer as well as the transversal dimensions of the guiding channel are fundamental requirements to ensure the success of the design. Besides, due to the dependence of the refractive index on wavelength, the evanescent field distribution is strongly affected by the dispersion characteristics of the polymeric optical waveguides.

Traditionally, polymeric planar optical waveguides were fabricated with different materials as guiding region: Polyvinyl alcohol (PVA), Poly (methyl methacrylate) (PMMA), Styrene acrylonitrile (SAN), etc. are typical examples [1–4]. Different techniques have been used to calculate the refractive index and thickness of the polymeric guiding layer; however, all proposals have been applied only to multimode optical waveguides [5, 6]. The fabrication of MZI with polymeric optical waveguides requires previous processes on the polymer before the final guide is obtained. In fact, in most cases, the polymer must be dissolved before deposition as well as subjected to UV exposure, heated and polished after being injected or spun to form the guiding region. Thus, the real refractive index and, consequently, the dispersion characteristics of the polymer are different from those provided by the manufacturer.

This paper presents a procedure which provides the real refractive index of transparent materials capable of confining light. Besides, the method can be used for analyzing and designing monomode and multimode planar optical waveguides with step index profile, as polymeric planar optical waveguides on glass substrate. The analysis stage allows to know the effective indices of guided modes from the physical parameters of the guide while the design option provides the refractive index and thickness of planar waveguides and only requires the knowledge of the effective indices of the guided modes. In both cases, the theoretical strategy allows working at any wavelength, including cutoff wavelengths, unlike most methods. This condition is very important in order to get weakly guided optical fields with large evanescent tails for increasing the sensitivity of the optical sensor. For

this purpose, the theoretical algorithm includes a LSE and LSM modes formulation which provides a powerful electromagnetic modelization. The theoretical method was programmed in Matlab language and the simulation software package Olympios was used to verify the results provided by the formulation. A complete agreement was obtained.

Monomode and multimode polymeric planar optical waveguides were manufactured. In all cases, and for confining light, polymer thin films were fabricated on glass substrates by using the spin-coating technique [7]. PMMA and Norland Optical Adhesive 61 (NOA61) polymers were deposited on borofloat and soda-lime glass substrates, respectively, and the prism-film coupler technique [8] was implemented to measure the effective indices of the guided modes. The Metricon system was used to compare measurements. Experimental effective indices were introduced in the formulation, and refractive index and thickness of the guiding layer were evaluated. In order to verify the accuracy of the algorithm, the thickness of several samples was measured with a profilometer. In all cases, the theoretical and experimental results agree very well.

## 2. THEORY

Channel optical waveguides propagate hybrid modes, with six electromagnetic field components. When one of the components of the field is negligible compared to the others, the modes can be designated as LSE (Longitudinal Section Electric)-LSM (Longitudinal Section Magnetic) [9–11]. LSE and LSM modes, with respect to the horizontal interfaces ( $x$ - $z$  plane in Fig. 1), have the same fundamental component of electric field as TE and TM modes, respectively. This characteristic allows analyzing the electromagnetic propagation of planar optical waveguides using the LSE-LSM formulation. In our case, and from the experimental point of view, the electric field dominant component is imposed by the laser polarization. As our region of interest is free of sources, we can calculate  $E$  and  $H$  fields from Hertz's potentials [9].

In our case, we focus on planar optical waveguides with step-index profile and manufactured by polymer deposition on glass. The geometry that determines the electromagnetic field propagation is shown in Fig. 1, where  $n_s$ ,  $n_f$  and  $n_c$  represent the refractive indices of the substrate, polymeric guiding region and cover, respectively. Consequently,  $n_s$  and  $n_f$  are constant whereas the cover will be air; therefore, we take  $n_c = 1$ .

## 2.1. Single Mode Planar Optical Waveguides

### 2.1.1. LSM Modes

According to the coordinate system shown in Fig. 1, we can express the electromagnetic field components from a Hertz's potential vector of electric type,  $\vec{M}_e$ , whose spatial dependence can be written as:

$$\vec{M}_e = \phi^e(x, y) e^{-\gamma z} \vec{a}_y \quad (1)$$

where  $\gamma$  represents the propagation constant in the  $z$  direction, and can be written in the following way:

$$\gamma = \alpha + jk_z \quad (2)$$

being  $\alpha$  the attenuation constant and  $k_z$  the phase constant in the  $z$  direction.

Assuming a lossless waveguide ( $\alpha = 0$ ), and since the three waveguide regions in Fig. 1, are infinite in the  $x$  direction, there is only variation in the  $y$  coordinate. Consequently, we can write the Helmholtz's equation, as follows:

$$\nabla_t^2 \phi^e(y) + (n^2 k_0^2 - k_z^2) \phi^e(y) = 0 \quad (3)$$

where  $\nabla_t^2$  represents the transverse component of the Laplacian operator and  $k_0$  the phase constant in the free space.

The potential scalar solutions  $\phi^e(y)$ , in Equation (3) can be written as [12]:

$$\phi^e(y) = \begin{cases} Ae^{-\eta_0 y} & y \geq 0 \\ B \cos k_y y + C \sin k_y y & -b \leq y \leq 0 \\ De^{\eta_1(y+b)} & y \leq -b \end{cases} \quad (4)$$

being  $\eta$ ,  $k_y$ ,  $\eta_1$  the transverse propagation constants in the respective regions: air, guiding layer and substrate.

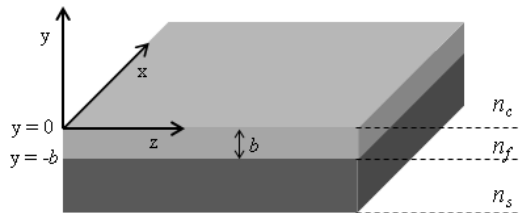


**Figure 1.** Scheme of a step-index planar optical waveguide with a guiding region with refractive index,  $n_f$ , and thickness,  $b$ . The cover of the waveguide is air and the substrate is a material with refractive index  $n_s$ .

Substituting the solutions of the Equation (4) in the differential Equation (3), we obtain the relationships that verify the refractive indices and the propagation constants in each region of the optical waveguide, as shown:

$$k_z^2 = n_s^2 k_0^2 + \eta_1^2 = n_f^2 k_0^2 - k_y^2 = k_0^2 + \eta_0^2 = n_{eff}^2 k_0^2 \quad (5)$$

where  $n_{eff}$  represents the effective refractive index of a guided mode in the direction propagation  $z$ .

In order to calculate the  $A$ ,  $B$ ,  $C$  and  $D$  constants in Equation (4), boundary conditions are applied to the electromagnetic field components, which are tangential to the interfaces. In the specific case of LSM modes,  $E_z$  and  $H_x$  are the tangential components given by the following equations [9]:

$$E_z = -j \frac{k_z}{n^2} \frac{\partial \phi^e(y)}{\partial y} \quad (6)$$

$$H_x = -\omega \varepsilon_0 k_z \phi^e(y) \quad (7)$$

where  $n$  represents the refractive index,  $\omega$  is the angular frequency, and  $\varepsilon_0$  refers to permittivity in vacuum.

After applying the continuity of the  $E_z$  and  $H_x$  components at  $y = 0$  and  $y = -b$ , we have the characteristic equation for LSM modes:

$$\eta_0 \cos k_y b - \frac{k_y}{n_f^2} \sin k_y b + \frac{\eta_1}{n_s^2} \cos k_y b + \frac{\eta_0 \eta_1 n_f^2}{n_s^2 k_y} \sin k_y b = 0 \quad (8)$$

In order to obtain the analytical expression that gives the thickness,  $b$ , and taking into account the fact that the tangent function is periodic every  $\pi$  radians, we can express  $b$  from Equation (8), as follows:

$$b = \frac{\tan^{-1} \left( \frac{\eta_0 n_s^2 + \eta_1}{n_s^2 k_y - \eta_0 \eta_1 n_f^4} \right) n_f^2 k_y}{k_y} \pm \frac{m\pi}{k_y} \quad (9)$$

where  $m = 0, 1, 2, \dots$  is any natural number.

From Equations (5) and (9), we obtain the following relationship:

$$b = \frac{\tan^{-1} \left( \frac{(n_s^2 \sqrt{n_{eff}^2 - 1} + \sqrt{n_{eff}^2 - n_s^2}) n_f^2 \sqrt{n_f^2 - n_{eff}^2}}{n_s^2 (n_f^2 - n_{eff}^2) - n_f^4 \sqrt{n_{eff}^2 - 1} \sqrt{n_{eff}^2 - n_s^2}} \right)}{\frac{2\pi}{\lambda_0} \sqrt{n_f^2 - n_{eff}^2}} \pm \frac{m\pi}{\frac{2\pi}{\lambda_0} \sqrt{n_f^2 - n_{eff}^2}} \quad (10)$$

Equation (10) relates the thickness,  $b$ , and the refractive index,  $n_f$ , of the guiding region.

For monomode waveguides, we have designed an iterative process that consists of assigning values to  $n_f$ , by successive increments,  $\Delta n$ . In

this way, and for each value of  $m$ , we can find a series of pairs,  $(n_f, b_f)$ , which represent the mathematical solutions of Equation (10). This iterative process is based on the guided propagation conditions:  $n_f > n_{eff} > n_s$  and it is applied as follows:

*First guided propagation condition ( $n_f > n_{eff}$ )*

Evidently, if a guided mode exists, it must verify  $n_f > n_{eff}$ . So,  $n_{eff}$  is the lower limit of  $n_f$ . Therefore, we can express  $n_f$  in the following way:

$$n_f^i = n_f^j + \Delta n \quad (11)$$

where  $i$  represents each iteration, being  $i = j + 1$ .

For the first iteration:  $i = 1$  and  $j = 0$ ; therefore, Equation (11) becomes:

$$n_f^0 = n_{eff} \quad (12)$$

*Second guided propagation condition ( $n_{eff} > n_s$ )*

On the other hand,  $n_{eff} > n_s$ , so that the index increment,  $\Delta n$ , can be calculated as follows:

$$\Delta n = \frac{n_{eff} - n_s}{D} \quad (13)$$

where  $D$  is a natural number that allows to fix the calculation accuracy.

When the calculation stops, a series of  $i$ -pairs  $(n_f^i, b^i)$  is obtained for each value of  $m$ . Each pair solution  $i$  provides the same effective refractive index,  $n_{eff}$ , which was evaluated experimentally for LSM polarization modes.

### 2.1.2. LSE Modes

For this family of modes, we operate in a similar way. We can express the electromagnetic field components from a Hertz's potential vector of magnetic type,  $\vec{M}_h$ . Since we are studying LSE modes, we apply the continuity of the  $E_x$  and  $H_z$  components at  $y = 0$  and  $y = -b$ . These components can be written as [9]:

$$E_x = \omega \mu_0 k_z \phi^h \quad (14)$$

$$H_z = -jk_z \frac{\partial \phi^h}{\partial y} \quad (15)$$

Following the same procedure as for LSM modes, we obtain the characteristic equation for LSE modes:

$$\eta_1 \cos k_y b + \frac{\eta_0 \eta_1}{k_y} \sin k_y b + \eta_0 \cos k_y b - k_y \sin k_y b = 0 \quad (16)$$

Taking into account the same considerations as for LSM modes, we can write the thickness,  $b$ , of the guiding layer and for LSE modes as follows:

$$b = \frac{\tan^{-1} \frac{(\eta_0 + \eta_1)k_y}{k_y^2 - \eta_0 \eta_1}}{k_y} \pm \frac{p\pi}{k_y} \tag{17}$$

where  $p = 0, 1, 2, \dots$  is any natural number.

From Equations (5) and (17), we obtain the following relationship:

$$b = \frac{\tan^{-1} \frac{(\sqrt{n_{eff}^2 - 1} + \sqrt{n_{eff}^2 - n_s^2})\sqrt{n_f^2 - n_{eff}^2}}{(n_f^2 - n_{eff}^2) - \sqrt{n_{eff}^2 - 1}\sqrt{n_{eff}^2 - n_s^2}}}{\frac{2\pi}{\lambda_0}\sqrt{n_f^2 - n_{eff}^2}} \pm \frac{p\pi}{\frac{2\pi}{\lambda_0}\sqrt{n_f^2 - n_{eff}^2}} \tag{18}$$

Equation (18) is solved by applying the iterative process described for LSM modes. Finally, we get a series of  $j$ -pairs,  $(n_f^j, b^j)$  for each value of  $p$ , so that each pair  $j$  provides the same effective index,  $n_{eff}$ , which was evaluated experimentally for LSE polarization modes.

Therefore, we have two sets of solutions: a set of  $i$ -pairs,  $(n_f^i, b^i)$ , for LSM modes, and a set of  $j$ -pairs,  $(n_f^j, b^j)$ , for LSE modes. Only the same pair solution,  $(n_f, b)$ , appears simultaneously in both sets of solutions. In other words, only this pair provides, simultaneously, the effective indices measured for the LSM and LSE modes supported by the same single mode planar optical waveguide. This pair is the only element of the intersection of both sets of solutions and represents the authentic physical solution in which we are interested.

Such a solution pair can be obtained graphically, by representing the two sets of solutions obtained for LSM and LSE modes. For each couple of values,  $m$  and  $p$ , we get two curves that intersect at one point. These intersections are mathematical solutions of the thickness and the refractive index of the guiding layer. The pair  $(n_f, b)$  which represents the correct physical solution is obtained by the intersection of the LSM and LSE curves that gives the smallest positive thickness,  $b$ .

## 2.2. Multimode Planar Optical Waveguides

### 2.2.1. LSM Modes

For multimode waveguides, Equation (10) is verified for each LSM guided mode. If the waveguide propagates  $r$  modes, we have a set of  $n_{eff_s}$  ( $s = 1, 2, 3, \dots, r$ ) effective refractive indices. Consequently, Equation (10) becomes in a system of  $r$  equations with the same thickness,  $b$ , and same refractive index,  $n_f$ . Substituting in

Equation (10) any two values of  $n_{effs}$  obtained experimentally for example  $s = i$  and  $s = j$ , and equating both expressions in  $b$ , the following relation is verified:

$$\begin{aligned} & \frac{\tan^{-1} \frac{(n_s^2 \sqrt{n_{effi}^2 - 1} + \sqrt{n_{effi}^2 - n_s^2}) n_f^2 \sqrt{n_f^2 - n_{effi}^2}}{n_s^2 (n_f^2 - n_{effi}^2) - n_f^4 \sqrt{n_{effi}^2 - 1} \sqrt{n_{effi}^2 - n_s^2}}}{\frac{2\pi}{\lambda_0} \sqrt{n_f^2 - n_{effi}^2}} \pm \frac{m_i \pi}{\frac{2\pi}{\lambda_0} \sqrt{n_f^2 - n_{effi}^2}} \\ & = \frac{\tan^{-1} \frac{(n_s^2 \sqrt{n_{effj}^2 - 1} + \sqrt{n_{effj}^2 - n_s^2}) n_f^2 \sqrt{n_f^2 - n_{effj}^2}}{n_s^2 (n_f^2 - n_{effj}^2) - n_f^4 \sqrt{n_{effj}^2 - 1} \sqrt{n_{effj}^2 - n_s^2}}}{\frac{2\pi}{\lambda_0} \sqrt{n_f^2 - n_{effj}^2}} \pm \frac{m_j \pi}{\frac{2\pi}{\lambda_0} \sqrt{n_f^2 - n_{effj}^2}} \quad (19) \end{aligned}$$

Equation (19) can be solved by using the bisection method. For different values of  $m_i$  and  $m_j$ , and from Equations (19) and (10), we get a set of mathematical pairs solutions  $(n_f^{(i,j)}, b)$ , corresponding to the refractive index and thickness of the guiding layer. However, in our method, the pair  $(n_f, b)$  which represents the correct physical solution is obtained when  $m_i$  and  $m_j$  represent the order,  $s$ , of the two guided modes.

### 2.2.2. LSE Modes

For LSE modes, the solution of  $(n_f, b)$  is obtained in a similar way. In this case, and using Equation (18) for thickness  $b$ , the relation to be solved by the bisection method has the form:

$$\begin{aligned} & \frac{\tan^{-1} \frac{(\sqrt{n_{effi}^2 - 1} + \sqrt{n_{effi}^2 - n_s^2}) \sqrt{n_f^2 - n_{effi}^2}}{(n_f^2 - n_{effi}^2) - \sqrt{n_{effi}^2 - 1} \sqrt{n_{effi}^2 - n_s^2}}}{\frac{2\pi}{\lambda_0} \sqrt{n_f^2 - n_{effi}^2}} \pm \frac{p_i \pi}{\frac{2\pi}{\lambda_0} \sqrt{n_f^2 - n_{effi}^2}} \\ & = \frac{\tan^{-1} \frac{(\sqrt{n_{effj}^2 - 1} + \sqrt{n_{effj}^2 - n_s^2}) \sqrt{n_f^2 - n_{effj}^2}}{(n_f^2 - n_{effj}^2) - \sqrt{n_{effj}^2 - 1} \sqrt{n_{effj}^2 - n_s^2}}}{\frac{2\pi}{\lambda_0} \sqrt{n_f^2 - n_{effj}^2}} \pm \frac{p_j \pi}{\frac{2\pi}{\lambda_0} \sqrt{n_f^2 - n_{effj}^2}} \quad (20) \end{aligned}$$

This formulation can be applied to monomode and multimode optical waveguides, unlike other methods, and provides additional important advantages in comparison with other proposals. For monomode waveguides, only two values of  $n_{eff}$  are necessary, one for each polarization (LSM and LSE); while, for multimode waveguides, we need to measure  $n_{eff}$  for each guided mode only in one polarization (LSM or LSE).

### 3. SIMULATION

In order to validate the theoretical formulation described above, it is necessary to solve Equations (10) and (18) (monomode waveguides) and (19) or (20) (multimode waveguides) which provide the unknowns,  $n_f$  and  $b$ . For this purpose, the algorithm was computed in Matlab. To test the applicability of the LSM and LSE formulation as well as the accuracy of the algorithm, the Effective Index Method [13–15] was used in the simulation software package Olympios. Monomode and multimode polymeric planar optical waveguides were simulated. Table 1 contains the simulation results for monomode waveguides: SI01, SI02 and SI03, and multimode samples: SI04 and SI05.

#### 3.1. Monomode Waveguides

Firstly, the polymeric monomode planar optical waveguides, labelled as SI01, SI02 and SI03, were simulated by Olympios. Assuming  $\lambda_0 = 632.8 \text{ nm}$  and  $n_s = 1.4699$ , this software package was used for obtaining the effective refractive indices. Table 1 contains the proposed input data,  $n_f^{\text{O}}$  and  $b^{\text{O}}$ , to Olympios, and the obtained effective refractive indices for LSM and LSE modes. Subsequently, and in order to obtain the refractive index,  $n_f^{\text{M}}$ , and the thickness,  $b^{\text{M}}$ , of the guiding layer, the output data,  $n_{eff}^{\text{LSM}}$  and  $n_{eff}^{\text{LSE}}$ , provided by Olympios, are used as input data for the LSM/LSE formulation, which was programmed in Matlab.

**Table 1.** Input and output data from Olympios (O) which were used to check the algorithm developed in Matlab (M). The agreement between the input data in Olympios and the output data from Matlab is shown.

Sample	Olympios Input Data		Olympios Output Data and Matlab Input Data		Matlab Output Data	
	$n_f^{\text{O}}$	$b^{\text{O}}$ ( $\mu\text{m}$ )	$n_{eff}^{\text{LSM}}$	$n_{eff}^{\text{LSE}}$	$n_f^{\text{M}}$	$b^{\text{M}}$ ( $\mu\text{m}$ )
SI01	1.490	1.2	1.4784	1.4791	1.490	1.2
SI02	1.480	0.9	1.4699	1.4700	~1.480	0.92
SI03	1.480	0.92	1.4699	1.4701	1.480	0.92
SI04	1.560	2.0	1.5538	1.5542	1.560	2.0
			1.5358	1.5370		
			1.5105	1.5115		
SI04	1.560	3.0	1.5570	1.5571	1.560	3.0
			1.5481	1.5485		
			1.5335	1.5344		
			1.5144	1.5156		

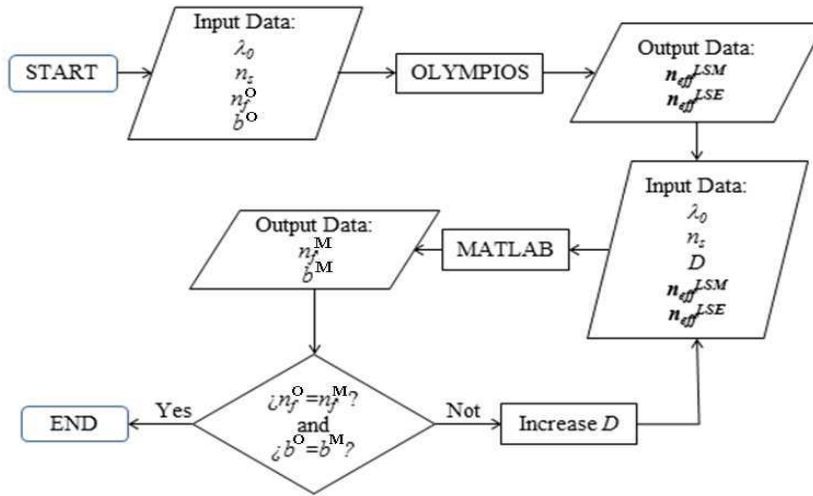


**Figure 2.** Flowchart for complete numerical simulation. The formulation programmed in Matlab is verified by the Olympios software package.

Last column in Table 1 shows the results obtained by the algorithm for  $n_f^M$  and  $b^M$ . In all cases, the proposed values of  $n_f^O$  and  $b^O$  as input data for Olympios agree exactly with the output data,  $n_f^M$  and  $b^M$ , obtained from Matlab. Fig. 2 outlines the complete flow of the simulation.

Using the iterative process explained in the previous section, the algorithm provides a graph with the possible mathematical solutions of  $n_f$  and  $b$ . These solutions are the intersection points of the LSM and LSE curves obtained for each couple of  $m$  and  $p$  values. This is shown in Fig. 3 for sample SI01.

Each curve corresponds to each value of  $m$  and  $p$ , in Equations (10) and (18), for LSM and LSE formulation, respectively. Therefore, for each pair  $(m, p)$  we obtain two curves which intersect at the solution point. However, the correct solution of  $n_f$  and  $b$  is provided by the intersection point of the LSM and LSE curves that gives the smallest positive thickness,  $b$ . In the case of sample SI01, this condition is verified when  $m = p = 1$ , as the inserted zoom shows in Fig. 3. The calculated refractive index and thickness for sample SI01 were:  $n_f = 1.490$  and  $b = 1.2 \mu\text{m}$ , which match to the input data of Olympios. We have used the same procedure for several samples, and we have achieved satisfactory results. In general,  $m$  and  $p$  have the same value;

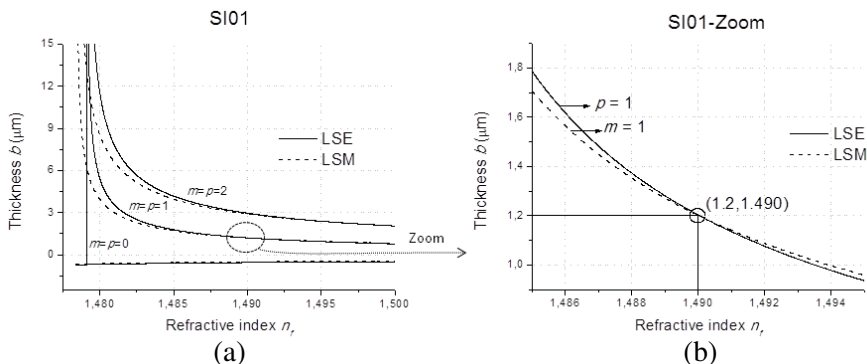


**Figure 3.** (a) Thickness,  $b$ , as a function of refractive index,  $n_f$ , for the sample SI01 and for several  $m$  and  $p$  values. These physical solutions are obtained when  $m = p = 1$  and they correspond to the intersection point  $(1.490, 1.2)$ . (b) Inserted zoom.

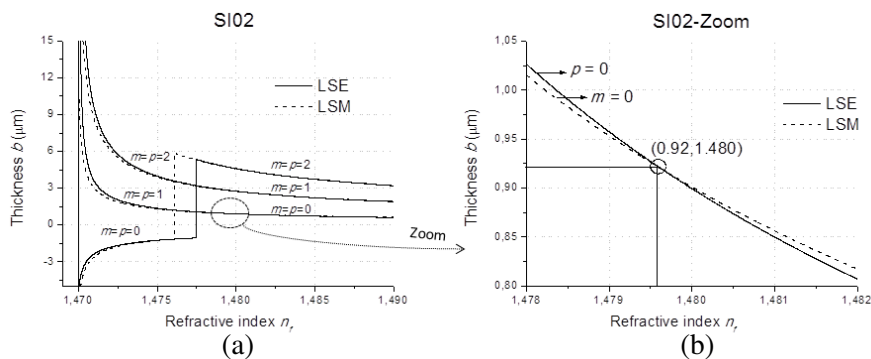


**Figure 4.** (a) Thickness,  $b$ , as a function of refractive index,  $n_f$ , for the sample SI02 and for several  $m$  and  $p$  values. These physical solutions are obtained when  $m = p = 0$  and they correspond to the intersection point  $(1.4796 \cong 1.48, 0.9)$ . (b) Inserted zoom.

however, when the guided modes are near to the cutoff wavelength,  $m$  and  $p$  can be different. In fact, the LSE and LSM formulation demonstrates there are three possible regions for solution in the case of monomode guides, two regions in which  $m$  and  $p$  are equal and a third region, which separates the two above, in which the indices  $m$  and  $p$  are different. This is shown in Fig. 4 and Fig. 5 for samples SI02 and SI03. In both cases, the correct solution is obtained for  $m = 0$ ,  $p = 0$  and  $m = 1$ ,  $p = 0$ , respectively.

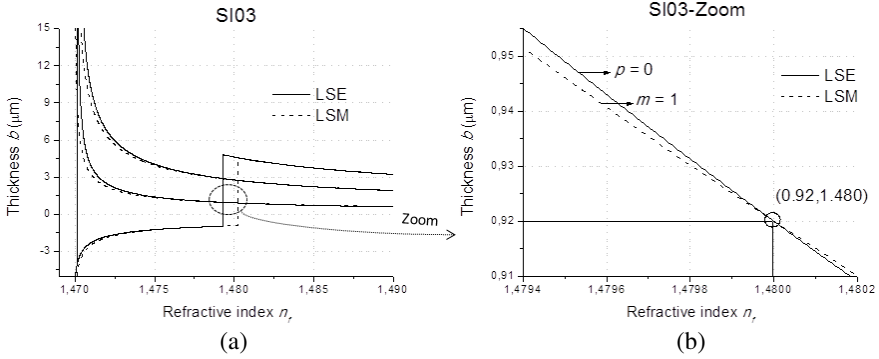


**Figure 5.** (a) Thickness,  $b$ , as a function of refractive index,  $n_f$ , for the sample SI03 and for several  $m$  and  $p$  values. These physical solutions are obtained when  $m = 1$ ,  $p = 0$  and they correspond to the intersection point  $(1.480, 0.92)$ . (b) Inserted zoom.

### 3.2. Multimode Waveguides

Once the theoretical formulation was successfully checked for monomode planar optical waveguides, we have applied it to multimode waveguides simulation. The flowchart is the same as shown in Fig. 2

Table 1 contains the input data,  $n_f^O$  and  $b^O$ , used in Olympios for the simulation of the samples SI04 and SI05 that we have chosen as example. In this case, the additional input data for Olympios were:  $\lambda_0 = 632.8$  nm,  $n_s = 1.5105$ . Table 1 shows the effective refractive indices,  $n_{eff}^{LSM}$  and  $n_{eff}^{LSE}$ , obtained for the simulated multimode planar optical waveguides, SI04 and SI05. Then, the algorithm developed in Matlab was checked for these multimode waveguides by introducing as data input the obtained effective indices and the rest of parameters:  $\lambda_0 = 632.8$  nm,  $n_s = 1.5105$  and  $D$ , which allows to fix the accuracy of calculation by the bisection method. By applying the process that we have explained for multimode waveguides, the algorithm directly returns the values of  $n_f$  and  $b$ . As shown in Table 1, the output values obtained with the algorithm are the same that the data input in the simulation software Olympios. A variety of multimode planar waveguides were fabricated and characterized. In all cases, we have achieved satisfactory results.

## 4. FABRICATION AND EXPERIMENT EVALUATION

### 4.1. Monomode Waveguides

Borofloat glass substrates ( $n_s = 1.4699$  at  $\lambda_0 = 632.8$  nm) and the PMMA polymer ( $n_f = 1.49$  at  $\lambda_0 = 632.8$  nm) were used to manufacture single-mode optical waveguides. Different thicknesses of the polymer were deposited on the glass using spin-coating system (WS-400A-6NPP, Laurell Technologies Corporation, USA).

The complete manufacturing process takes place in a controlled environment room, with humidity 50% and temperature 20°C. The glass substrates were conditioned in the first step. Then, the polymer was deposited on the substrate. Different spin speed and several layers of polymer overlapping were used to manufacture monomode optical planar waveguides with different thickness,  $b$ . In all cases, the resulting sample was heated to 250°C for 5 minutes on a hot plate. In this way, the PMMA was firmly adhered to the glass.

In order to test monomode regime, the next step was the experimental characterization of the manufactured samples. For this, we have implemented a prism-film coupling technique [6]. The setup, fully automated, is shown in Fig. 6. To excite the guided modes, we have used a SF11 prism with a refractive index  $n_{\text{prism}} = 1.779$  at  $\lambda_0 = 632.8$  nm, and with an angle  $\varphi_{\text{prism}} = 45^\circ$ . The effective refractive index,  $n_{\text{eff}}$ , of each guided mode was calculated by using the

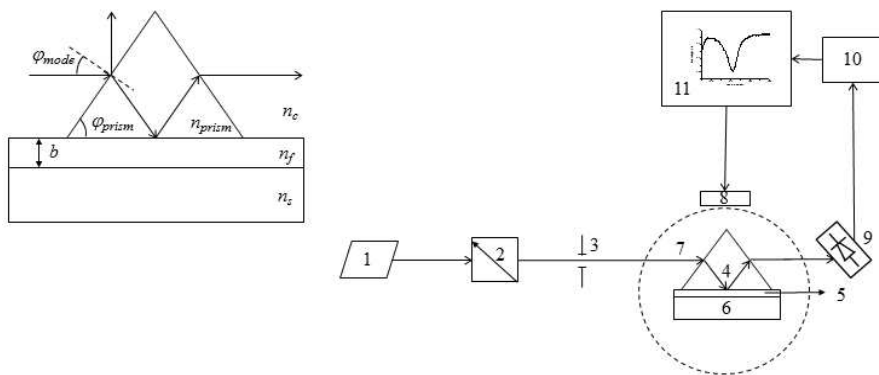


**Figure 6.** Prism-coupling technique setup: 1-Laser, 2-Polarizer, 3-Diaphragm, 4-Prism, 5-Polymer-thin film, 6-Glass substrate, 7-Goniometer, 8-Piezoelectric movement system, 9-Optical detector, 10-Data acquisition system, 11-Computer.

equation [8]:

$$n_{eff} = n_{prism} \sin \left[ \varphi_{prism} + \sin^{-1} \left( \frac{\sin \varphi_{mode}}{n_{prism}} \right) \right] \quad (21)$$

being  $\varphi_{mode}$  the incidence angle with respect to the normal of the prism, for which there is a guided mode. This angle was measured with a motorized goniometer (Physik Instrumente, Germany), which allows a precision of  $0.0001^\circ$ . The light coming from the laser (Uniphase He-Ne 1100, USA) is properly polarized to LSM (TM) or LSE (TE) with the help of a linear polarizer (Optosci, Scotland). A diaphragm is used for improving the coupling of the light. The coupling prism and the optical waveguide, as well as an optical detector (DET110, Germany), are attached to the axis of the goniometer. In order to optimize de light coupling, the complete set is placed on two superimposed translation stages (Oriel, USA), with perpendicular movement relative to one another, and to the axis of rotation of the goniometer. The rotation of the complete set is provided by a piezoelectric movement system (Physik Instrumente, Germany). The light exiting the prism is collected by the optical detector and a data acquisition system (HP 34970A, USA) provides the intensity light data for each incident angle. All functions are controlled by computer.

Measurements of the effective refractive index for monomode samples, and for LSM and LSE polarizations, were taken. As example, the sample PM26 was chosen as a reference for this paper. This sample was manufactured with three PMMA layers, as can be seen in Fig. 7(a)

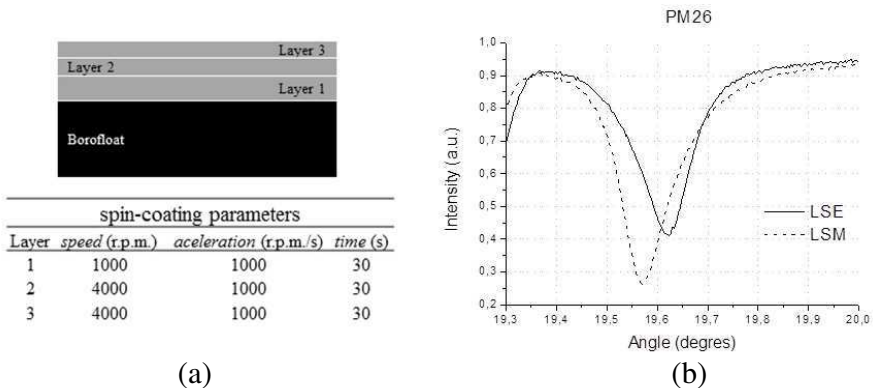


**Figure 7.** (a) Scheme of the cross-section view for the PM26 sample. The spin-coating parameters, for each layer of PMMA, are included. (b) Angle measurements obtained for the sample PM26, and LSM-LSE polarizations, by using the prism-coupling method.

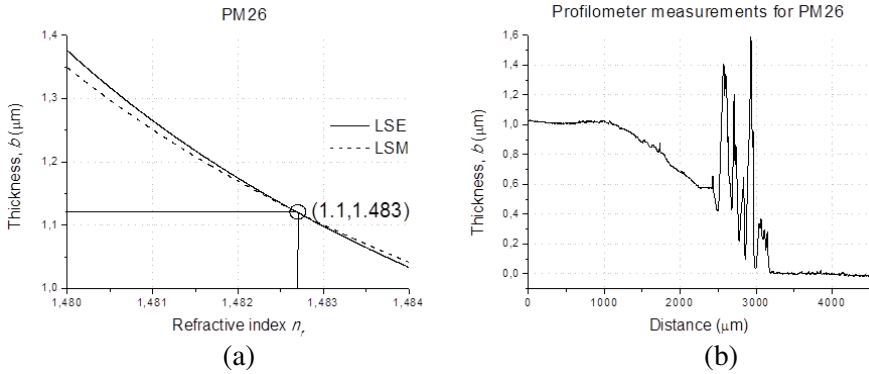


**Figure 8.** (a) Thickness,  $b$ , as a function of refractive index,  $n_f$ , for the monomode sample PM26. These physical solutions are obtained when  $m = p = 1$  and they correspond to the intersection point (1.1, 1.483). (b) Measurements of the thickness,  $b$ , as a function of distance, obtained with the profilometer for the sample PM26.

For this optical waveguide, Fig. 7(b) shows the measurements of the incidence angle for LSM and LSE polarizations. The minimum of each curve corresponds to the angle of incidence,  $\varphi_{\text{mode}}$ , which causes a LSM and LSE guided mode. Using Equation (21), the effective refractive index had been calculated for both polarizations, obtaining the following results:  $n_{\text{eff}}^{\text{LSM}} = 1.4723$  and  $n_{\text{eff}}^{\text{LSE}} = 1.4728$ . The Matlab algorithm was applied for calculating the refractive index,  $n_f$ , and the thickness,  $b$ , of the polymer in sample PM26. As input data were used:  $n_{\text{eff}}^{\text{LSM}} = 1.4723$ ,  $n_{\text{eff}}^{\text{LSE}} = 1.4728$ ,  $\lambda_0 = 632.8 \text{ nm}$ ,  $n_s = 1.4699$  and  $D = 1000$ . Fig. 8(a) shows the results provided by the algorithm for the sample PM26. The refractive index and thickness for this sample were:  $n_f = 1.483$  and  $b = 1.1 \mu\text{m}$ .

Finally, a profilometer (Veeco Dektak Surface Profilometer, Germany) was used to verify the thickness results provided by the algorithm. In order to allow this measurement, a piece of tape was located over the glass substrate before depositing the polymer. Then, the piece of tape was removed, obtaining a step discontinuity between the surface of the glass substrate and the polymer layer. Several thickness measurements were taken in each sample by using a profilometer around the step discontinuity, and in different regions. Fig. 8(b) shows the average of three measurements on the sample PM26. As we can observe, the thickness measured using the profilometer was  $b = 1.0 \mu\text{m}$ . The most important parts in the graph are the beginning and the end of the measurement. The

central part of the experimental graph shows a high level of noise introduced by the discontinuity glass surface-polymer. Comparing the profilometer measurement with the results provided by the algorithm, we can observe just a difference of  $0.1 \mu\text{m}$ . We have used the same procedure for a variety of monomode waveguides. In all cases, the same agreement between theory and measurements was obtained.

## 4.2. Multimode Waveguides

Soda-lime glasses substrates ( $n_s = 1.5105$  at  $\lambda_0 = 632.8 \text{ nm}$ ) and the photopolymer Norland Optical Adhesive 61 (NOA61) ( $n_f = 1.56$  at  $\lambda = 632.8 \text{ nm}$ ) were used to manufacture multimode optical waveguides. Different thicknesses of the polymer were deposited on the glass using the spin-coating technique.

The manufacturing process was performed following the environment conditions used for monomode waveguides. In order to obtain different thicknesses in the polymeric layer, the viscosity of the NOA61 was modified and deposited on the substrate in three different ways: a) without changing the viscosity; b) heating the polymer at  $90^\circ\text{C}$  just before to spin the sample; c) in a dissolution of acetone (NOA61: Acetone (1 : 2)) In all cases, after depositing the polymer, we have done a UV exposure during 1 hour using a  $365 \text{ nm}$  UV lamp (LTF Labortechnik, Germany), followed by a postbake at  $60^\circ\text{C}$  for 12 hours, in a thermally controlled oven (Digitheat from J. P. Selecta, Spain). In this way, the NOA61 was firmly adhered to the glass.

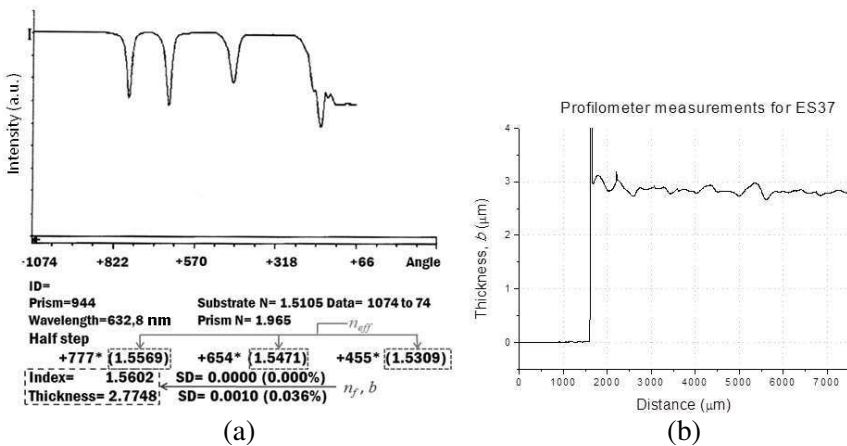


**Figure 9.** (a) Measurements for the multimode planar optical waveguide ES37, and for LSE polarization, obtained by using the MetriCon system. (b) Measurements of the thickness,  $b$ , as a function of distance, obtained with the profilometer for the sample ES37.

The next step was the experimental characterization of the manufactured samples. For measuring the effective indices of the guided modes, we have used the same prism-coupling system developed for monomode waveguides characterization. The Metricon prism coupler equipment, installed at the University of Santiago de Compostela (Spain), was used to measure the effective indices and compare them with those obtained by the designed prism-coupling system. Furthermore, the Metricon predicts the refractive index,  $n_f$ , and thickness,  $b$ , of the guiding layer, allowing comparison with the theoretical results provided by the algorithm. In all cases, the agreement was excellent.

The sample ES37 was chosen as a reference for this paper. This optical waveguide was manufactured with NOA61 which was heated at 90°C before spinning the polymer. Fig. 9(a) shows the measurements of the effective indices obtained with the Metricon system, for the three guided modes and LSE polarization. The obtained experimental results were:  $n_{eff1}^{LSE} = 1.5569$ ,  $n_{eff2}^{LSE} = 1.5471$  and  $n_{eff3}^{LSE} = 1.5309$ , as well as a refractive index,  $n_f = 1.560$  and a thickness,  $b = 2.8 \mu\text{m}$ . By using the experimental effective indices as data input, the Matlab algorithm was executed for calculating the refractive index,  $n_f$ , and the thickness,  $b$ , of the sample ES37. The theoretical results provided by the algorithm were:  $n_f = 1.560$ , and  $b = 2.8 \mu\text{m}$ , which show an excellent agreement with the experimental ones provided by the Metricon system.

Finally, the profilometer was used to verify experimentally the thickness,  $b$ , calculated by the algorithm. In order to allow this measurement, half of the sample was immersed in acetone inside an ultrasonic system, to remove a part of the polymer over the substrate. Fig. 9(b) shows the average of the measurements for the sample ES37. As for monomode waveguides, the central part of the graph shows a high peak of noise due to the glass-polymer discontinuity, which is obtained when removing the polymer. In this case, the measured average thickness,  $b$ , using the profilometer is around  $2.8 \mu\text{m}$ , which agrees very well with the value provided by the Metricon and with the theoretical result given by the proposed formulation. In order to further investigate the behavior of the algorithm, additional samples were manufactured and tested. In all cases, the same agreement between theory and measurements was obtained.

## 5. CONCLUSIONS

The theoretical procedure presented in this work provides the refractive index of transparent materials, capable of being deposited as a solid

thin layer on glass for confining light. The method combines a LSM and LSE modes formulation with a specific calculation algorithm and allows the analysis and design of monomode and multimode planar optical waveguides with step refractive index profile. Effective refractive indices (analysis) as well as the refractive index and thickness of the guiding layer (design) of monomode and multimode planar optical waveguides can be obtained with high accuracy. With respect to other traditional methods, this strategy has the following advantages: a) only requires the experimental evaluation of the effective indices of the guided modes and can be applied to monomode and multimode planar optical waveguides, including zones around the cutoff wavelength; b) the refractive index-wavelength dependence, as well as the thickness, of any guiding layer material can be evaluated; and c) only requires low-cost lab equipment, avoiding expensive optical characterization systems. The theoretical performance and accuracy of the procedure was verified by using the commercial software package Olympios. Polymeric planar optical waveguides on glass substrate were fabricated and characterized, both theoretically and experimentally. The prism-film coupler method and the Metricon equipment were used for effective indices measurements and for comparison. Refractive index and thickness of monomode and multimode polymeric thin films on glass substrate were evaluated. A profilometer was used for the measurement of the guiding layer thickness. In all cases an excellent agreement was obtained between theory and experiments.

## ACKNOWLEDGMENT

This work have been developed under sponsorship and support from a scholarship granted “Severo Ochoa” by FICYT (Principado de Asturias, Spain) with reference BP09-007 and by the MICINN (Government of Spain) under project CTQ2011-25814. Special thanks to Jesús Liñares from de University of Santiago de Compostela (Spain) for the measures with the Metricon system.

## REFERENCES

1. Qurechi, G. J., V. K. Gupta, et al., “Four layer polymeric optical waveguides based on styrene acrylonitrile (SAN),” *Proceedings of SPIE*, Vol. 4679, 440–444, 2002.
2. Ghawana, K., S. Singh, and K. N. Tripathi, “Determination of waveguide parameters of acrylonitrile-based polymer optical waveguides,” *Journal of Optics*, Vol. 29, No. 4, 265–267, 1998.

3. Kumar, R., A. P. Singh, et al., "Fabrication and characterization of polyvinyl-alcohol-based thin-film optical waveguides," *Optical Engineering*, Vol. 43, No. 9, 2134–2142, 2004.
4. Ren, Y., "Efficiency shifts of prism coupling into polymer waveguides subject to environmental variations," *Optical Materials*, Vol. 19, No. 4, 443–447, 2002.
5. Kersten, R. T., "Numerical solution of the mode-equation of planar dielectric waveguides to determine their refractive index and thickness by means of a prism-film coupler," *Optics Communications*, Vol. 9, No. 4, 427–431, 1973.
6. Ulrich, R. and R. Torge, "Measurement of thin film parameters with a prism coupler," *Applied Optics*, Vol. 12, No. 12, 2901–2908, 1973.
7. Luurtsema, G. A., "Spin coating for rectangular substrates," M. Sc. Thesis, Department of Electrical Engineering and Computer Sciences, University of California, Berkeley, July 1997.
8. Ulrich, R., "Theory of the prism-film coupler by plane-wave analysis," *Journal of the Optical Society of America*, Vol. 60, No. 10, 1337–1350, 1970.
9. Itoh, T., "Dielectric waveguide-type millimeter-wave integrated circuits," *Infrared and Millimeter Waves*, Vol. 4, 199–271, K. J. Button, J. C. Wiltse, Editors, Academic Press, New York, 1981.
10. Young, L. and H. Sobol, "Advances in microwaves," Vol. 8, Academic Press, New York, 1974.
11. Collin, R. E., *Foundations for Microwave Engineering*, 2nd Edition, McGraw-Hill, New York, 1992.
12. Hunsperger, R. G., "Integrated optics: Theory and technology," *Springer Series in Optical Sciences*, 3rd Edition, Vol. 33, T. Tamir, Editor, Springer-Verlag, Berlin, 1991.
13. Marcatili, E. A. J., "Dielectric rectangular waveguide and directional coupler for integrated optics," *Bell System Technical Journal*, Vol. 48, No. 7, 2071–2102, 1969.
14. Toullos, P. and R. Knox, "Rectangular dielectric imagelines for millimeter integrated circuits," *Western Electronic Show and Convention*, 25–28, Los Angeles, California, 1970.
15. Suhara, T., Y. Handa, et al., "Analysis of optical channel waveguides and directional couplers with graded-index profile," *Journal of Optical Society of America*, Vol. 69, No. 6, 807–815, 1979.